Indian Journal of Pure & Applied Physics
Vol. 52, November 2014, pp. 776-782

Comparative analysis of the millimeter wave performance of diamond based IMPATT diode with that of SiC (4H) IMPATT diode

B Chakrabarti[1], D Ghosh[2,*] & M Mitra[3]

[1]Department of ECE, Bengal Institute of Technology, Kolkata 150, India

[2]Department of ECE, Future Institute of Engineering & Management, Kolkata 150, India

[3]Dept. of E&TC Engineering, Bengal Engineering & Science University, Shibpur, Howrah 711 103, W Bengal, India

*E-mail: dg1036@gmail.com

Received 16 January 2013; revised 30 September 2013; accepted 3 July 2014

A detailed comparative analysis of the diamond semiconductor based DDR IMPATT devices in W-band has been carried out (normal and photo illuminated) through a simulation scheme. The simulation results reveal that an optimized unilluminated diamond IMPATT diode of efficiency 18.45% can be realized, whereas 4H-SiC IMPATT can have efficiency of 11.97%. Under optical illumination, the admittance and negative resistance values of the IMPATT diode degrade due to additional photo generated carriers. The negative conductance (–G) and total negative resistance ($-Z_R$) of the diamond based DDR IMPATT diode decrease by 7.03% and 8.5%, respectively when the diode is exposed to photo illumination whereas, for SiC based diode the decrements are 6.06% and 6.09%, respectively. Moreover under optical illumination, the quality factor (Q_p) of diamond IMPATT increases by 22.5% and it is only 6.5% for SiC based devices. Therefore, from the simulation work it is well established that, though the photosensitivity of 4H-SiC based IMPATT is better than its diamond counterpart the overall small signal performance of the illuminated diamond IMPATT degrades far more than SiC based devices due to very high reported carrier ionization rates in diamond. The simulation results also reveal the superiority of diamond based IMPATT device in terms of heat sink design in comparison to 4H-SiC based devices.

Keywords: Diamond IMPATT, Silicon carbide IMPATT, Negative resistivity, Heat sink, Photosensitivity

1 Introduction

To meet the gradual demand of high power and high frequency two terminals solid state sources which can operate at high temperature the use of wide band gap semiconductors such as gallium nitride (GaN) and silicon carbide (SiC) for microwave and millimeter wave power applications have been discussed by many researchers[1-7]. High value of breakdown voltage is required for high power generation, while high value of thermal conductivity is also necessary for good thermal stability of the device. The interest in diamond as high power microwave and millimeter wave source has grown with the improvements in epitaxial growth, rectifying and ohmic contacts. Fujimori *et al*[8]., Okano *et al*[9]. have led to renewed interest in developing diamond devices that will work at high temperature and high frequency. Moreover, with the advent of diamond CVD process[10] and etching technology[11] it become possible to fabricate diode with diamond as the base material. Diamond is recognized as having many superior material properties for possible future electronic devices, such as high breakdown field, high saturation velocity, and high carrier mobilities and highest thermal conductivity of all materials. A comparison of electronics and thermal properties of some common semiconductors is presented in Table 1. The mobilities of diamond are very high with only the electron mobility of GaAs exceeding those values. High carrier mobilities are desirable for fast response and high frequency electronic devices. High thermal conductivity is very suitable for power electronics devices which suffer from a high generation of heat. For traditional power devices, heat sinks have to be included in the structure to prevent the device from malfunction. For diamond devices that may not necessary malfunction as it has the highest thermal conductivity. As a wide band gap semiconductor, diamond has the benefit of thermal stability and a high break down field which determines the maximum field strength and the material can withstand without breakdown. Diamond also offers many additional advantages over other wide band gap semiconductor materials such as gallium nitride (GaN) and silicon carbide (SiC). The growth of the epitaxial layer of diamond in a CVD process is in

Table 1 — Comparison of the properties of various semiconductors

Material	Si	GaAs	4H-SiC	GaN (Wz)	Diamond
Bandgap (E_g) (ev)	1.1	1.4	3.2	3.4	5.5
Breakdown field (E_c) (MV/cm)	0.3	0.4	3	5	20
Electron mobility (μ_n) (cm^2/V-s)	1450	8500	900	2000	4500
Hole mobility(μ_p) (cm^2/V-s)	480	400	120	200	3800
Thermal conductivity (W/cm-k)	1.5	0.55	3.7	1.3	24
Saturation velocity of electron (v_{ns}) ($\times 10^7$ cm/sec)	1	1	2	2.2	1.2

many ways simpler than it is to grow for other wide band gap semiconductor materials. This is due to the simpler structure of diamond, consisting of carbon atoms only. Again polyatomic materials such as SiC and GaN require careful control of the stoichiometry and they exist in many hundred different crystalline structures. Epitaxy of SiC is riddled with a particular problem, the formation of tubular channels, called micro pipes[12] during growth. This problem does not exist for diamond. Another advantage associated with growing diamond in a CVD process is that the raw materials are cheap as compared to SiC and GaN. The first ever millimeter wave performance of diamond IMPATT was simulated and compared with that of conventional Si, GaAs, and InP IMPATT at different mm wave frequency bands by Trew *et al*[13]., which established the superiority of diamond based IMPATT in terms of efficiency and output power. Later Tao Wu[14] has also analyzed the performance of diamond IMPATT in the terahertz frequency band taken into consideration different diode structures.

However, detailed small signal and *dc* analysis results of diamond based IMPATT diode are not available in the current literature which is very much necessary considering the future prospect of diamond as mm-wave power source. The authors, in the present paper, have done the simulation studies on diamond based DDR IMPATT diode at W-band (75 GHz-110 GHz) and compared the performance with that of SiC counterpart. Some experimental[15] and theoretical[3,4] studies on the optically illuminated IMPATT diode revealed the degradation in performance in terms of output power and efficiency of the diode.

The authors have also performed detailed study on diamond IMPATT diode under optical illumination and compared the results with that of SiC based diode. Taking into consideration the poor efficiency and larged c power dissipation at the junction of IMPATT diode, it is required that the diode has to be mounted on a very good heat sink substance for thermal stability.

The use of diamond as heat sink for traditional power devices has been discussed by many researchers[16-18]. The superior performance of diamond IMPATT diode in terms of physical dimension and cost of the heat sink is also discussed in the present paper.

2 Simulation Methodology and Material Parameters

For the present analysis, a flat-profile DDR (n^{++}, n, p and p^{++}) structure is considered, where n^{++} and p^{++} are highly doped substrates and cap layers, respectively and n is the epilayer. In the *dc* method, the numerical computation starts at the field maximum near the metallurgical junction. The method is used by simultaneous solving Poisson and carrier current continuity equations at each point in the depletion layer. The *dc* electric field and normalized carrier currents density profile in the depletion layer are obtained by a double –iterative simulation technique described elsewhere[3]. The field boundary conditions are given as:

$$E(-W_n)=0 \text{ and } E(W_p)=0 \quad \ldots(1)$$

where $-W_n$ and W_p represent the edges of the depletion layer in n and p regions, respectively.

The boundary conditions for normalized current density $P(x)$, are given as:

$$P(-W_n)=(2/M_p-1) \text{ and}$$

$$P(W_p)=(1-2/M_n) \quad \ldots(2)$$

where $M_n = J/J_{ns}$, $M_p = J/J_{ps}$, J_{ns} and J_{ps} are electron and hole leakage current densities, respectively. M_n and M_p are hole and electron current multiplication factors, respectively. Again $P=(J_p-J_n)/J$, where J_p is the hole current density, J_n the electron current density and J is the total current density. The breakdown voltage of the diode is obtained by integrating the electric field profile over the entire depletion layer width, that is:

$$V_B = \int_{-W_n}^{W_p} E(x)\mathrm{d}x \quad \ldots(3)$$

The *dc* to mm wave conversion efficiency is calculated from the approximate formula:

$$\eta\ (\%) = (V_D)*(100/\pi)/V_B \quad \ldots(4)$$

where V_D is the voltage drop across the drift region. Also $V_D = V_B - V_A$, where V_A is the voltage drop across the avalanche region.

In the simulation method, the authors have considered latest reported values of material parameters and their realistic variation with electric field and temperature. The field dependent electron and hole ionization rates[19] for 4H-SiC are incorporated into the present analysis. The temperature dependent drift velocity and mobility of charge carriers[20] in 4H-SiC have been used in the computation process. The Monte Carlo simulated values of drift velocity and mobility of charge carriers[21,13] in diamond are considered for the simulation experiment. Because of the lack of experimental values of ionization coefficients in diamond the authors have considered the theoretical predicted values[13] in the present study.

The range of frequencies over which the diode exhibits negative conductance can easily be computed by Gummel-Blue method[22]. The resistive part $R(x, \omega)$ and reactive part $X(x, \omega)$ are obtained by splitting the diode impedance $Z(x, \omega)$ using Gummel-Blue method and thus two different equations are framed[3]. Then, by using modified Runga-Kutta method[23], the solutions of these two equations are found following a double iterative simulation scheme. The small signal parameters like negative conductance ($-G$), susceptance (B), impedance (Z) of the diode and the range of frequencies over which the diode exhibits negative conductance are found after satisfying the boundary conditions derived elsewhere[24-26].The diode total negative resistance ($-Z_R$) and reactance ($-Z_x$) at a particular frequency can be determined from numerical integration of the resistivity [$-R(x)$] and reactivity [$-X(x)$] profiles over the entire depletion layer.

Thus

$$-Z_R = \int_{-W_n}^{W_p} -R\,dx \text{ and } -Z_X = \int_{-W_n}^{W_p} -X\,dx \quad \ldots(5)$$

The diode total impedance Z is obtained by:

$$Z_{total} = \int_{-W_n}^{W_p} Z(x,\omega)\,dx = -Z_R + jZ_x \quad \ldots(6)$$

The diode admittance is expressed as :

$$Y = 1/Z = -G + jB = 1/(-Z_R + jZ_x)$$

and diode total negative conductance and susceptance have been calculated from the following formulas:
or $G = -Z_R/[(Z_R)^2 + (Z_x)^2]$

and

$$B = Z_x/[(Z_R)^2 + (Z_x)^2] \quad \ldots(7)$$

G and B are both normalized to the diode area.

The Avalanche (resonance) frequency (f_a) is a frequency at which the imaginary part, susceptance (B) of the admittance changes its nature from inductive to capacitive. The small signal quality factor (Q_p) is defined as the ratio of the imaginary part of the admittance (B) to the conductance (G) at the peak frequency, i.e.

$$-Q_p = (B_p/-G_p) \quad \ldots(8)$$

when the IMPATT diode is exposed to interstellar radiation, the performance of IMPATT oscillator changes appreciably due to the absorption of optical photon of energy greater than the band gap energy of the semiconductor. The photo generated minority carriers add up with temperature generated minority carriers and thereby enhance the total leakage current that alters the avalanche phase delay of the diode and modifies the performance of the diode.

Normally, the leakage current (J_s) under reverse bias condition is due to the thermally generated electrons and holes.Therefore:

$$J_s = J_{ns}(th) + J_{ps}(th) \quad \ldots(9)$$

So the current multiplication factors at the two edges of the depletion layers are given as:

$$M_{n/p} = J/[J_{ns}(th) \text{ or } J_{ps}(th)] \quad \ldots(10)$$

where J is the bias current density. Therefore, $M_{n/p}$ can be considered almost infinity. Thus, the enhanced leakage current under optical illumination lowers the magnitude of $M_{n/p}$.

Under optical illumination, the electron current multiplication factor changes to:

$$M_n = J_o/[J_{ns}(th)+J_{ns}(opt)] \quad \ldots(11)$$

where $J_{ns}(opt)$ is the leakage current due to photo generated electrons.

Similarly, the hole current multiplication factor under optical illumination is given as:

$$M_p = J_o/[J_{ps}(th)+J_{ps}(opt)] \quad \ldots(12)$$

where J_{ps} (opt) is the leakage current due to photo generated holes.

Simulation studies have been carried out by many researchers[3,4] to study the effects of optical illumination on the dynamic properties of SDR IMPATT diode based on high band gap materials such as SiC and GaN. In the present paper, the authors have studied the performance of diamond DDR IMPATT diode under optical illumination and compared its performance with that of SiC (4H) DDR IMPATT diode. As the diamond has very narrow optical absorption band and very large band gap energy (5.45 eV), it is expected that lesser number of photo generated minority carriers would be produced in diamond compared to SiC. In our analysis, we have considered M_n=100 for diamond and M_n=25 for SiC.

The design of IMPATT diodes as high power microwave and millimeter wave source involves the realization of high thermal conductance structures. Techniques to increase the thermal conductance include mounting the wafer on a heat sink, minimizing contact metallization thickness, and choosing high thermal conductivity material for the heat sink. An ordinary Mesa diode over diamond/copper heat sink is shown in Fig. 1.

The thermal resistance can be defined as R_{th} = temperature change/heat flow rate.

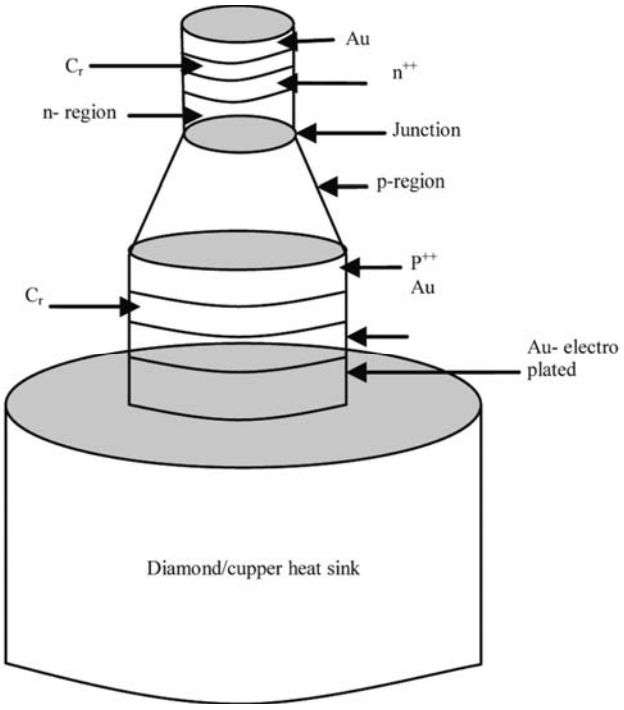

Fig. 1 — MESA diode structure

Thermal resistance of a cylindrical block can be formulated as:

$$R_{th}=\left(\frac{L}{AK}\right)$$

where $A= \pi r^2$ (cylinder having circular cross-section of radius r), L is the length of the cylinder and k is the conductivity of the material.

The total thermal resistance of the diode below the junction (towards heat sink) can be written as :

$$R_{diode\_down}= R_p + R_{p+} + R_{contact\_down} \quad \ldots(13)$$

Thermal resistance of the heat sink will be:

$$R_{heat\_sink} = \left(\frac{L_H}{\pi R_H^2 K_H}\right) \quad \ldots(14)$$

where L_H, $R_{H,}$ and K_H are the heat sink thickness, radius and conductivity, respectively. In the thermal analysis, the junction temperature around 500 K is considered as the safe temperature of operation for both the diodes.

3 Results and Discussion

The optimized design parameters of the diamond and SiC DDR IMPATT diodes are summarized in Table 2. The *dc* and high frequency simulation results of the diode under both illumination and no illumination cases are given in Table 3. It can be observed that the value of the peak electric field (E_m) at the junction is about 3 times larger in case of SiC IMPATT diode as compared to diamond diode. In addition to it, the active layer widths (*n* and *p* region) are greater in case of SiC IMPATT diode which resulted ten times higher value of breakdown voltage (V_B) in SiC diode as compared to diamond. Considering smaller values of ionization rate coefficients (α_n and α_p) in SiC compared to diamond under the same operating current density, the

Table 2 — Design parameters

Diode Type	Width of *n* region (W_n) (μm)	Width of *p* region (W_p) (μm)	Doping conc (*n* region) (10^{23} m^{-3})	Doping conc (*p* region) (10^{23} m^{-3})	Current density (10^8 Am^{-2})
SiC-4H	2.4	2.4	0.18	0.2	1
Diamond	0.930	0.812	0.31	0.33	1

Table 3 — Small signal and *dc* results for diamond and 4H-SiC Impatt diode

Diode type	M_n	M_p	E_m ($Vm^{-1}10^8$)	V_B (V)	H (%)	f_p (GHz)	G_p ($10^6 Sm^{-2}$)	Z_R ($10^{-8}\Omega m^{2)}$	Q
SiC (4H)	10^6	10^6	2.31	919	11.97	93	–0.264	–0.279	36.7
	25	10^6	2.30	917	12.24	93	–0.248	–0.262	39.1
Diamond	10^6	10^6	0.936	92.6	18.45	104	–8.39	–4.43	1.2
	100	10^6	0.935	91.6	18.51	105	–7.80	–4.07	1.47

avalanche region is less localized in SiC diode which reduces the diode efficiency in SiC as compared to diamond and the same can be verified from Table 3.Taking into account the effect of optical illumination, it is observed that the efficiency of both type of diodes increases slightly. The negative conductance is an important parameter that determines the amount of *RF* power which can be generated by the IMPATT diode. It can be seen from Table 3 that the peak negative conductance ($-G_p$) for diamond diode is approximately 30 times higher than that for SiC devices. Diamond IMPATT diode also gives better performance as compared to SiC diode in terms of total negative resistivity ($-Z_{RP}$) of the device. Again looking into the quality factor (Q_p) of the diode it has been seen that diamond IMPATT gives better response than SiC based diode. Therefore, considering the *dc* and small signal properties of the diode it can be concluded that diamond IMPATT diode gives improved response in comparison with its SiC counterpart. Figures 2 and 3 show the conductance ($-G$) versus susceptance (B) plot, respectively for both the diodes under illumination and non-illumination conditions. The small signal data given in Table 3 indicate that under optical illumination the peak negative conductance ($-G_P$) decreases by 6.06 % for SiC diode whereas it reduces by 7.03 % in case of diamond diode. The same trend can also be reflected from Figs 2 and 3. There is upward shift by 1 GHz in the value of peak operating frequency (f_p) in diamond diode when the diode is exposed to photo illumination whereas no such shift can be seen in SiC diode. The negative resistivity profile R(x) at the optimum frequency which provides better insights into the region of depletion layer that contributes *RF* power is shown in Figs 5 and 6, respectively. The computed $R(x)$ profile in each case is characterized by two negative resistivity peaks (R_{max}) almost in the middle of the drift layers. It can further be verified that the magnitude of the negative resistivity peak in the hole drift region (p-region) is appreciably higher compared with that of the peak at

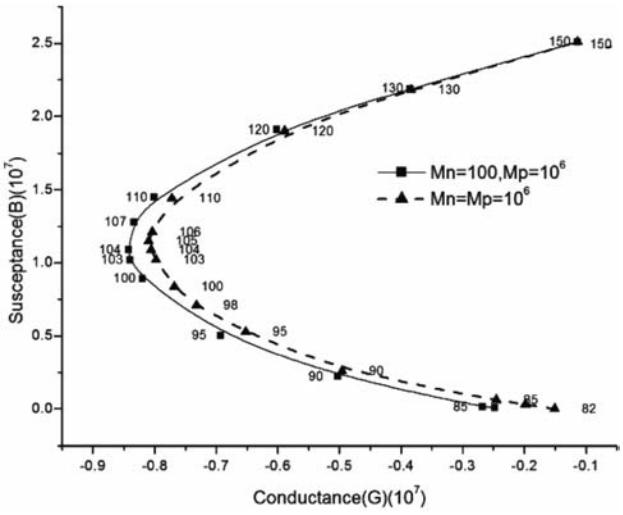

Fig. 2 — Conductance (G) versus susceptance (B) plot for diamond DDR IMPATT diode under normal and illuminated conditions

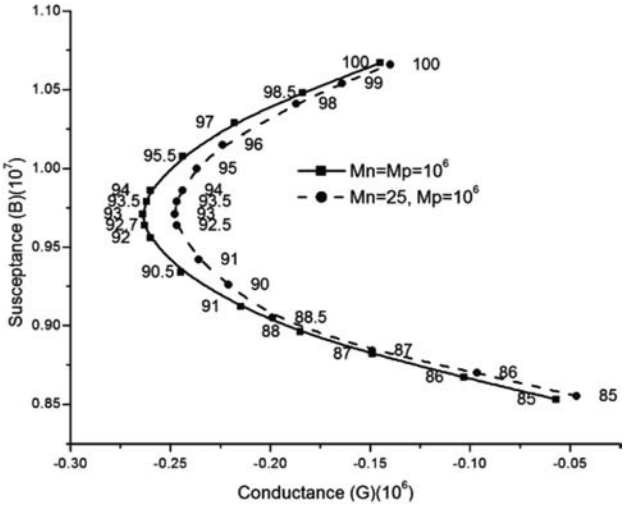

Fig. 3 — Conductance (G) versus susceptance (B) plot for SiC DDR IMPATT diode under normal and illuminated conditions

electron drift region (n-region) for SiC diode whereas no such perceptible difference can be observed in the case of diamond diode.

Figures 4 and 5 also exhibit that due to variation of M_n the negative resistivity peaks are lowered in

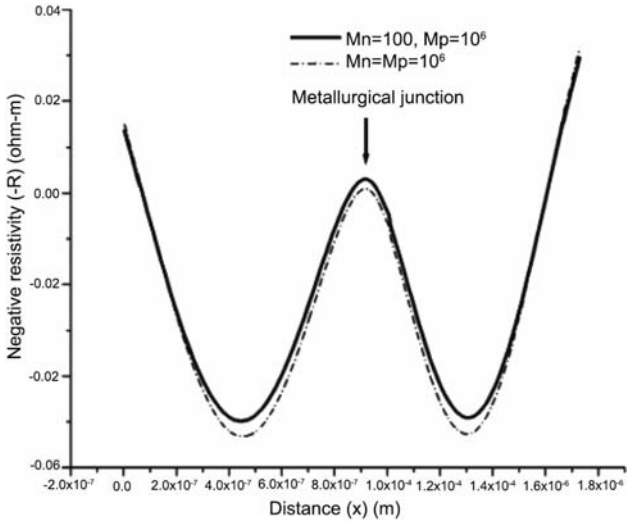

Fig. 4 — Plot of negative resistivity of illuminated and unilluminated conditions for diamond IMPATT diode

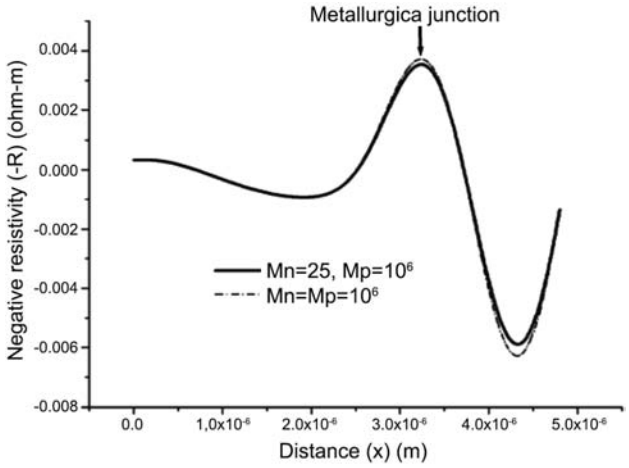

Fig. 5 — Plot of negative resistivity of illuminated and unilluminated conditions for 4H-SiC IMPATT diode

magnitude accompanied by a gradual shift in their positions from the middle of the drift region towards the n^{++} and p^{++} edges. Under optical illumination, the total negative resistivity value decreases by 8.5% for diamond diode and by 6.09% for SiC diode. This may be due to very high ionization rate of charge carriers in diamond which produce large number of ionizing carriers rapidly causing the avalanche phase delay to change[15]. In addition to it, the quality factor (Q_p) of diamond IMPATT increases by 22.5% whereas it is only 6.5% for SiC diode as M_n decreases.Therefore, it can be predicted that the small signal performance of the diamond IMPATT diode would be degraded more severely as compared to SiC diode when the diode is exposed to interstellar radiation.

Table 4 — Comparative analysis of the heat sink requirement

Diode type	Heat sink Material	Heat sink dimension		Thermal resistance (°C/watt)	Junction temperature (K)
		Diameter (μm)	Thickness (μm)		
4H-SiC	Diamond	900	700	2.76	515
Diamond	Cupper	280	700	29.47	514

Table 4 presents a comparative analysis of the required heat sink of the designed diodes. The high input power and low efficiency of SiC diode causes large *dc* power to dissipate at the junction. Therefore, for good thermal design SiC IMPATT diode requires diamond heat sink of diameter (D_H) = 900 μm and width L_H=700 μm (Table 4). Whereas copper heat sink of diameter (D_H) = 560 μm and width L_H=700 μm are required for the safe operation of diamond DDR diode. Therefore, considering physical dimension and cost of the heat sink a diamond IMPATT diode can give better performance as compared to SiC based IMPATT devices.

4 Conclusions

The suitability of diamond based IMPATT as a high power mm-wave source has been thoroughly investigated for the first time. The investigation revealed that IMPATTs fabricated from diamond may exhibit superior mm-wave performance as compared to similar devices fabricated from SiC. This paper reveals that, as a high power millimeter wave source diamond based IMPATT device is more a potential candidate than its SiC counterpart. The small signal performance in terms of total negative resistance, negative conductance and quality factor is found to degrade with the enhancement of leakage current by electron dominated photo current. However, the effect of optical illumination on diamond based IMPATT diodes are found to be more intense than that of the 4H-SiC based diodes. Optimum design of heat sink is an essential requirement for steady and safe operation of IMPATT oscillators. Taking into consideration the cost of the system, typical heat sink designs are presented in this paper by using both diamond (high cost) and copper (comparatively low cost).

References

1 Mehdi I, Haddad G I & Mains R K, *Journal Appl Phys*, 64(3) (1988) 1533.
2 Buniatyan V V & Aroutiounian V M, *Journal Phys D: ApplPhys*, 40 (2007) 6355.
3 Mukherjee M, Mazumder N, Roy S K &Goswami K, *SemicondSci Technology (UK)*, 22 (2007) 1258.

4 Mukherjee M, Mazumder N & Roy SK, *IEEE Trans on Device and Material Reliability*, 8 (2008) 608.
5 Chakrabarti B, Ghosh D &Mitra M, *Int J Eng Sci Technology*, 3 (2011) 6153.
6 GhoshD,Chakrabarti B & Mitra M, *Int J Scientific Engineering Research*, 3 (2012) 355.
7 Pattanaik S R, Dash G N & Mishra J K, *Semicond Sci Technol*, 20 (2005) 299.
8 Fujimori N, Imai T & Doi A, *Vaccum (Science Direct)*, 36 (1986)99.
9 Okano K, Naruki H, Akiba Y, Kurosu T, Lida M, & Hirose Y, *Japan J Appl Phys*, 27 (1988) L173-5.
10 May P W, *Phil Trans R Soc Lond*, 358 (2000) 473.
11 Hwang D S, Saito T & Fujimori N, *Diamond and Related Materials*, 13 (2004) 2207.
12 Dmitriev V, Rendakova S, Kuznetsov N, Savkina N, Andreev A, Rastegeava M, Mynbaeva M & Morozov A, *Materials Science and Engineering*, B 61-62 (1999) 446.
13 Trew R J, Yan J B & Mock P M, *Proc IEEE*, 79 (1991) 598.
14 Wu T, *Int J Infrared Milli Waves*, 29 (2008) 634.
15 Vyas H P,Gutmann R J& Borrego J M, *IEEE Trans Elect Devices*, 26 (1979)232.
16 Decker D R &Schorr A J, *IEEE Trans Elec Devices*, ED-17(1970) 739.
17 Csanky G, *John Wiley &Sons Ltd*, 6 (1990) 73.
18 Leistner D, *IEE ProceedingsSolid-state and Electron devices*, 131 (1984) 56.
19 Loh W S, Ng B K & Ng J S, *IEEE Trans Electron Devices*, 55 (2008)1984.
20 Electronic Archive: New Semiconductor Materials, Characteristics and properties [online]. Available: http://www.ioffe.ru/SVA/NSM/Semicond/SiC.
21 Watanabe T, Teraji T, Ito T, Kamakura Y& Taniguchi K, *J Appl Phys*, 95 (2004) 4866.
22 GummelH K& Blue J L, *IEEE Trans Eletron Devices*, 14(1967) 569.
23 Roy S K, Banerjee J P &PatiS P, *Proc of NASACODE-IV Conf on Numerical Analysis of Semiconductor Devices: Dublin: Boole Press* (1985) 494.
24 Mukherjee M & Roy S K, *Current Appl Phys*, 10 (2010) 646.
25 De P, *Indian J Pure & Appl Phys*, 43 (2005) 794.
26 Eisele H & Haddad G I, *Active microwave Diodes in Modern Semiconductor Devices ed S M Sze,* John Wiley & Sons (New York), (1997) 343.